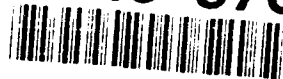


AD-A245 876



②

NAVAL POSTGRADUATE SCHOOL

Monterey, California



DTIC
ELECTE
FEB 14 1992
S D D

THESIS

HIGH-GAIN, HIGH-POWER FREE ELECTRON LASERS

by

Jung-Hyun Park

June, 1991

Thesis Advisor:

W. B. Colson

Approved for public release; distribution is unlimited

92-03537



UNCLASSIFIED

SECURITY CLASSIFICATION OF THIS PAGE

REPORT DOCUMENTATION PAGE				
1a. REPORT SECURITY CLASSIFICATION Unclassified			1b. RESTRICTIVE MARKINGS	
2a. SECURITY CLASSIFICATION AUTHORITY			3. DISTRIBUTION/AVAILABILITY OF REPORT Approved for public release; distribution is unlimited.	
2b. DECLASSIFICATION/DOWNGRADING SCHEDULE				
4. PERFORMING ORGANIZATION REPORT NUMBER(S)			5. MONITORING ORGANIZATION REPORT NUMBER(S)	
6a. NAME OF PERFORMING ORGANIZATION Naval Postgraduate School		6b. OFFICE SYMBOL (If applicable) 33	7a. NAME OF MONITORING ORGANIZATION Naval Postgraduate School	
6c. ADDRESS (City, State, and ZIP Code) Monterey, CA 93943-5000			7b. ADDRESS (City, State, and ZIP Code) Monterey, CA 93943-5000	
8a. NAME OF FUNDING/SPONSORING ORGANIZATION		8b. OFFICE SYMBOL (If applicable)	9. PROCUREMENT INSTRUMENT IDENTIFICATION NUMBER	
8c. ADDRESS (City, State, and ZIP Code)			10. SOURCE OF FUNDING NUMBERS	
			Program Element No	Project No
			Task No	Work Unit Accession Number
11. TITLE (Include Security Classification) HIGH-GAIN, HIGH-POWER FREE ELECTRON LASERS				
12. PERSONAL AUTHOR(S) PARK, JUNG-HYUN				
13a. TYPE OF REPORT Master's Thesis		13b. TIME COVERED From To	14. DATE OF REPORT (year, month, day) 1991 JUNE	15. PAGE COUNT 42
16. SUPPLEMENTARY NOTATION The views expressed in this thesis are those of the author and do not reflect the official policy or position of the Department of Defense or the U.S. Government.				
17. COSATI CODES			18. SUBJECT TERMS (continue on reverse if necessary and identify by block number)	
FIELD	GROUP	SUBGROUP	FEL, undulator, gain spectrum, gain evolution	
19. ABSTRACT (continue on reverse if necessary and identify by block number)				
<p>The LLNL Paladin FEL experiment is shown to exhibit clear and dramatic effects governed by the electron beam velocity distribution for the first time. The FEL integral equation is used to show that there is significant broadening of the gain spectrum due to the Gaussian velocity distribution, and also shows a plateau in the gain evolution along the undulator due to a triangular-shaped velocity distribution.</p> <p>The gain spectra and power evolution from simple, single-mode simulations are compared to the LLNL ELF experiments. The microwave power evolution along the undulator is compared as well for both the tapered and untapered undulators. In all cases, the agreement is found to be good.</p>				
20. DISTRIBUTION/AVAILABILITY OF ABSTRACT <input checked="" type="checkbox"/> UNCLASSIFIED/UNLIMITED <input type="checkbox"/> SAME AS REPORT <input type="checkbox"/> DTIC USERS			21. ABSTRACT SECURITY CLASSIFICATION Unclassified	
22a. NAME OF RESPONSIBLE INDIVIDUAL W. B. Colson			22b. TELEPHONE (Include Area code) (408) 646 2765	22c. OFFICE SYMBOL PH/CW

DD FORM 1473, 84 MAR

83 APR edition may be used until exhausted
All other editions are obsolete

SECURITY CLASSIFICATION OF THIS PAGE

UNCLASSIFIED

Approved for public release: distribution is unlimited.

HIGH-GAIN, HIGH-POWER FREE ELECTRON LASERS

by

Jung-Hyun Park

Captain, Republic of Korea Army

B. S., Korea Military Academy, 1985

Submitted in partial fulfillment of the
requirements for the degree of

MASTER OF SCIENCE IN PHYSICS

from the

NAVAL POSTGRADUATE SCHOOL

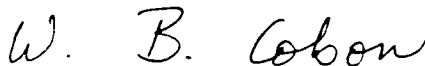
June 1991

Author:

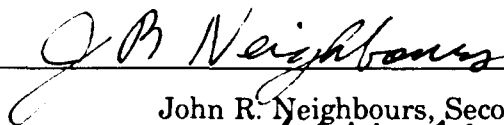


Jung-Hyun Park

Approved by:



William B. Colson, Thesis Advisor



John R. Neighbours, Second Reader



Karlheinz E. Woehler, Chairman,

Department of Physics

ABSTRACT

The LLNL Paladin FEL experiment is shown to exhibit clear and dramatic effects governed by the electron beam velocity distribution for the first time. The FEL integral equation is used to show that there is significant broadening of the gain spectrum due to the Gaussian velocity distribution, and also shows a plateau in the gain evolution along the undulator due to a triangular-shaped velocity distribution.

The gain spectra and power evolution from simple, single-mode simulations are compared to the LLNL ELF experiments. The microwave power evolution along the undulator is compared as well for both the tapered and untapered undulators. In all cases, the agreement is found to be good.

Accession For	
NTIS CRA&I	<input checked="" type="checkbox"/>
DTIC TAB	<input type="checkbox"/>
Unannounced	<input type="checkbox"/>
Justification	
By	
Distribution/	
Availability Codes	
Dist	Avail. and/or Special
A-1	

Table of Contents

I. INTRODUCTION	1
II. BASIC FEL THEORY	4
A. ELECTRONS IN THE UNDULATOR	4
B. OPTICAL FIELD EVOLUTION AND THE WAVE EQUATION	7
C. ELECTRON DYNAMICS AND THE PENDULUM EQUATION	9
III. BEAM QUALITY AND GAIN EVOLUTION	11
A. THE FEL INTEGRAL EQUATION	11
B. ELECTRON DISTRIBUTION FUNCTIONS	12
C. GAIN SPECTRUM BROADENING IN THE 5 m PALADIN	14
D. A PLATEAU IN THE GAIN EVOLUTION OF THE 15 m PALADIN	18
IV. SIMPLE MODEL OF THE ELF FEL	22
A. DESCRIPTION OF ELF EXPERIMENT	22
B. SIMPLE FEL EQUATIONS FOR ELF EXPERIMENT	23
C. RESULTS	26
LIST OF REFERENCES	33
INITIAL DISTRIBUTION LIST	35

ACKNOWLEDGEMENT

The author is grateful for support of this work by the Naval Postgraduate School, the U. S. Office of Naval Research, and the Republic of Korea Army. The author would also like to thank W. B. Colson for his invaluable assistance, loving wife, Kang, Jin-Hee, for her devotion and patience, and cute daughter, Jee-Hyun.

I. INTRODUCTION

In a Free Electron Laser (FEL), a relativistic high-quality beam of electrons, passing through an undulator magnet, generates a powerful and coherent electromagnetic wave [1]. Coherence may develop after many passages in the undulator, when the device operates as an oscillator, or in one passage in the amplifier configuration. The choice between an oscillator configuration and a amplifier configuration is generally determined by the accelerator that drives the FEL; specifically by the pulse format and peak current of the accelerator. Induction linear accelerators produce short pulses, usually 10-100 ns long, that are widely spread in time with high peak current. The pulses are too far apart to be synchronized with optical pulses in a resonator. To be interesting, the amplifier must have high gain in a single pass of the light through the amplifier. The high peak current of an induction linac permits both high gain and high efficiency, the fraction of electron beam energy converted to light.

The evolution of coherent electron bunching is the key element to any FEL gain mechanism. In a high-gain amplifier, like the Paladin FEL [2-4] at Lawrence Livermore National Laboratory (LLNL), maintaining coherence of the electron bunch over a significant interaction length imposes important restrictions on the initial electron beam quality. The design of an high gain FEL amplifier requires high beam current and a long undulator; both features tend to allow gain to be easily degraded by poor beam quality.

Paladin is the first short-wavelength FEL to operate in the high current regime where the growth mechanism is dominated by the longitudinal velocity distribution of the electron beam. It is observed that the growth of the optical power along the 15 m Paladin undulator is not exactly exponential, but is determined by the shape of electron distribution function. Similarly, the gain spectrum measured in the earlier 5 m long Paladin amplifier shows a dramatically broader and lower shape due to the electron beam distribution. The FEL integral equation [5-7] is used to calculate the optical field evolution in the presence of an arbitrary electron velocity distribution.

The LLNL Electron Laser Facility (ELF) FEL is a single-pass, high-gain, high-power amplifier operating in the microwave regime at 34.6 GHz frequency [8-11]. The characteristics of this FEL have been extensively studied with large simulations including many transverse modes, diffraction, beam emittance, and betatron focusing. A relatively simple, single-mode model of the FEL interaction using only the electron pendulum and optical wave equations can describe the most important features of the ELF FEL. The waveguide, used in the experiment to confine the natural diffractive spreading of the microwave beam, can be simply modeled by a filling factor and a shift in resonance.

The most significant contributions to the analysis of a high-gain, high-power FEL are summarized below.

- Gain spectrum broadening of the 5 m Paladin experiment due to poor beam quality are examined by FEL integral equation.

- Plateau in the 15 m Paladin FEL gain evolution is explored by the velocity distribution functions.
- The asymmetrical shape of high-gain ELF FEL is examined by simple FEL equations.
- Gain evolutions with both untapered and tapered ELF FEL are explored using simple FEL equations.

II. BASIC FEL THEORY

A. ELECTRONS IN THE UNDULATOR

In order to discuss the principles of the FEL, it is important to consider the individual electron trajectories in the undulator field alone, without the presence of light. The interaction between the negatively charged electrons is negligible in typical FELs [1], and the beam is focused externally before entering the undulator. Under the influence of the undulator magnetic field, the electrons will deflect periodically in the transverse direction, or "wiggle" as they travel along the optical mode axis. The ideal form of the on-axis helical undulator field at $x = y = 0$ is

$$\vec{B} = B[\cos(k_0 z), \sin(k_0 z), 0] \quad , \quad \text{for } 0 < z < L \quad , \quad (1)$$

where B is the peak undulator field strength, $k_0 = 2\pi/\lambda_0$ is the undulator wavenumber associated with the wavelength λ_0 , z is the distance along the longitudinal axis of the undulator, $L = N\lambda_0$ is the undulator length, and N is the number of undulator periods. The Lorentz force equations [12] become

$$\frac{d}{dt}(\gamma\vec{\beta}) = -\frac{e}{mc}(\vec{\beta} \times \vec{B}) \quad , \quad \text{and} \quad \frac{d\gamma}{dt} = 0 \quad , \quad (2)$$

where $\gamma = (1 - \vec{\beta}^2)^{-1/2}$ is the Lorentz factor, m is the electron rest mass, $e = |e|$ is the electron charge magnitude, c is the speed of light,

$\vec{\beta} = \vec{v}/c = \vec{\beta}_\perp + \vec{\beta}_z$, $\vec{\beta}_\perp$ is the perpendicular component which refers to the transverse direction, and $\vec{\beta}_z$ is the parallel component along the axis of undulator. We see that the electron energy, γmc^2 , is a constant of motion in the magnetic field above. Substituting (1) into (2) gives

$$\frac{d}{dt}(\gamma \vec{\beta}_\perp) = -\frac{e}{mc} \beta_z B [-\sin(k_0 z), \cos(k_0 z), 0] \quad (3)$$

The velocity can be solved exactly from (3), but assuming perfect injection, $\gamma \gg 1$, and $\beta_z \approx 1$, the velocity components can be written as

$$\vec{\beta}(t) = \left[\frac{K}{\gamma} \cos(k_0 ct), -\frac{K}{\gamma} \sin(k_0 ct), \beta_z \right] \quad (4a)$$

$$\text{where } \beta_z = \left[1 - \frac{1+K^2}{\gamma^2} \right]^{1/2} \quad (4b)$$

and $K = eB\lambda_0/2\pi mc^2$ is the dimensionless undulator parameter or vector potential.

The electron position can be found by an additional integration of (4a) and is

$$\vec{r}(t) = \left[-\frac{K\lambda_0}{2\pi\gamma} \sin(\omega_0 t), \frac{K\lambda_0}{2\pi\gamma} \cos(\omega_0 t), \beta_z ct \right] \quad ,$$

where $\omega_0 = \beta_z k_0 c$. In a typical FEL, $K = 1$, $\lambda_0 = 5$ cm, and $\gamma = 100$, so that the electrons travel at speed $\beta_z c \approx c$ along the z -axis for several meters while executing small transverse oscillations with amplitude $K\lambda_0/2\pi\gamma \approx 0.1$ mm, which is smaller than the typical beam radius. The transverse deflection of the highly relativistic electron beam in the alternating, periodic field of the undulator leads to spontaneous emission. Even if the deflection

is too small to be visualized on the scale of the undulator, it is still responsible for crucial spontaneous emission, and FEL gain.

The spontaneous emission mechanism is essentially classical, and can be described by the Larmor formula giving the total power emitted from a single electron as $P_e = 2e^2\gamma^4\dot{\beta}_\perp^2/3c \approx 2\gamma^2B^2cr_e^2/3$, where $r_e = e^2/mc^2$ is the classical electron radius (in cgs units) [12]. This radiation is emitted into a small cone about the forward direction with angular width $\approx \gamma^{-1}$. This narrow-spectrum radiation is trapped in the optical resonator and used to supply the starting photons for oscillator operation. The interaction between these photons with the electron beam in the undulator is the essential concept of FEL physics. In the amplifier configuration, the photons are supplied by the seed laser.

The fundamental feature of the FEL mechanism is that the beam electrons undergo axial bunching in the combined undulator and radiation fields to exchange energy with an optical field. Assuming a circularly polarized plane wave, the optical fields are taken to be [12]

$$\vec{E}_s = E(\cos \psi, -\sin \psi, 0) \quad , \quad \text{and} \quad \vec{B}_s = E(\sin \psi, \cos \psi, 0) \quad , \quad (5)$$

where E is the optical field strength, $\psi = kz - \omega t + \phi$ with carrier frequency $\omega = kc$, $k = 2\pi/\lambda$ is the optical wavenumber correlated with the wavelength λ , and ϕ is the optical phase.

Since the electron travels at slightly less than the speed of light, several optical wavelengths pass over an electron as it travels the full length of the undulator. When exactly one optical wavelength passes over an electron as

that electron travels through one undulator wavelength, resonance is established. Efficient energy exchange requires that the electrons experience near resonant forces from the optical and undulator fields. For $\gamma \gg 1$, this resonance is achieved when the optical wavelength, the beam energy, the undulator strength, and the undulator period approximately satisfy [1]

$$\lambda \approx \lambda_0 \frac{(1+K^2)}{2\gamma^2} .$$

The expression for the resonant FEL wavelength above shows one of the FEL's most important attributes, continuous tunability. As the electron energy from the accelerator is varied, or as the undulator strength K is varied, the resonant wavelength is changed.

B. OPTICAL FIELD EVOLUTION AND THE WAVE EQUATION

In order to follow the growth of the optical field it is necessary to develop a wave equation. Start with Maxwell's wave equation in the Coulomb gauge [12],

$$\left[\nabla^2 - \frac{1}{c^2} \frac{\partial^2}{\partial t^2} \right] \vec{A} = -\frac{4\pi}{c} \vec{J}_\perp ,$$

where \vec{A} is the optical vector potential, and \vec{J}_\perp is the transverse current density. An appropriate form of the vector potential for a circularly polarized optical wave is $\vec{A} = (E/k)[\sin \psi, \cos \psi, 0]$. The total current can be represented as the sum of the single-particle currents in the electron beam, $\vec{J}_\perp = -ec \sum \vec{\beta}_\perp \delta^{(3)}(\vec{r} - \vec{r}_i)$, where \vec{r}_i follows the trajectory of the i^{th} particle.

Assuming that the amplitude and phase of the optical field is taken to vary slowly over an optical period ($\dot{E} \ll \omega E, \dot{\phi} \ll \omega \phi$) and over an optical wavelength ($E' \ll kE, \phi' \ll k\phi$) and keeping only terms with single derivatives, the equation can be written as

$$\left[\frac{\partial}{\partial z} + \frac{1}{c} \frac{\partial}{\partial t} \right] E e^{i\phi} \approx -\frac{2\pi e K \rho}{\gamma} \langle e^{-i\zeta} \rangle, \quad \text{where } \zeta = (k_0 + k)z - \omega t,$$

ρ is the electron beam particle density, the brackets, $\langle \dots \rangle$, indicate a phase average over the sample electrons within a wavelength of light, and ζ is a dimensionless variable that describes the electron's phase with respect to the combined optical and undulator fields within roughly one optical wavelength, since $k \gg k_0$ and $z \approx \beta_z ct$. If we assume a long electron pulse and don't consider longitudinal optical modes, we can remove z -dependence from the wave equation, then the wave equation can be written as

$$\overset{\circ}{a} = -j \langle e^{-i\zeta} \rangle, \quad \text{for } 0 < \tau < 1, \quad (6)$$

where the complex dimensionless field envelope and current density are

$$a = \frac{4\pi e K L N E e^{i\phi}}{\gamma^2 m c^2}, \quad j = \frac{8N(e\pi K L)^2 \rho F}{\gamma^3 m c^2},$$

$F = r_b^2/w^2$ is the "filling factor" which is the ratio of the electron beam area, πr_b^2 , to the optical mode area πw^2 , averaged over the undulator length, $\tau = ct/L$ is the dimensionless time, and the " $\overset{\circ}{}$ " denotes a time derivative with respect to τ . If many electrons are randomly spread in longitudinal position, then the phase average $\langle e^{-i\zeta} \rangle \approx 0$, with no optical field growth. In order to understand the FEL interaction, first we must examine how

electrons evolve from their initial positions within a wavelength of light.

C. ELECTRON DYNAMICS AND THE PENDULUM EQUATION

The interaction of the electrons and the optical fields inside the undulator is described by the complete Lorentz force law and the energy equation [12];

$$\frac{d}{dt}(\gamma\vec{\beta}) = -\frac{e}{mc} [\vec{E} + (\vec{\beta} \times \vec{B})] , \quad (7a)$$

$$\text{and } \frac{d\gamma}{dt} = -\frac{e}{mc} \vec{\beta} \cdot \vec{E} . \quad (7b)$$

Inserting the full combined fields of the undulator field (1) and optical field (5), the transverse motion with perfect injection can be found to be

$$\vec{\beta}_\perp = -\frac{K}{\gamma} [\cos(k_0 z), \sin(k_0 z), 0] + \frac{A}{\gamma} [\sin \psi, \cos \psi, 0] , \quad (8)$$

where $A = eE\lambda/2\pi mc^2$ is related to the optical vector potential and is analogous to the definition of K .

From (7b) and (8), the change of electron's energy is found to be [1]

$$\dot{\gamma} = \frac{eEK}{\gamma mc} \cos(\zeta + \phi) . \quad (9)$$

The exchange of energy of the electrons is easily understood in terms of the electron's phase, ζ . For example, electrons with phases such that, $-\pi/2 < (\zeta + \phi) < \pi/2$, will get energy from the optical field causing them to accelerate. Other electrons with phases, $\pi/2 < (\zeta + \phi) < 3\pi/2$, will lose energy to the optical wave causing it to grow. For a random distribution of initial phases, about half the electrons gain energy and about half lose. But, under

the influence of the combined fields, the electrons will begin to "bunch" at desirable phases and cause gain during a pass down the undulator.

To further clarify the dynamics of the electrons in the undulator, it is convenient to rewrite (9) in terms of ζ alone. Using the relation $\gamma^2 = 1 - \beta_{\perp}^2 - \beta_z^2$, and the conditions $\gamma \gg 1$, $\beta_z \approx 1$, and $\beta_{\perp}^2 \approx K^2/\gamma^2$, it can be shown that the individual electrons follow motion described by a simple pendulum equation [1]

$$\ddot{\zeta} = \dot{v} = |a| \cos(\zeta + \phi) \quad , \quad (10)$$

where $v = \dot{\zeta} = L[(k + k_0)\beta_z - k]$ is the dimensionless phase velocity.

The wave equation (6) and the pendulum equation (10) are valid in both strong and weak optical fields with high or low gain. They are not accurate for the high-efficiency FEL where there are significant changes in the electron energy γmc^2 . The electron energy is treated as a constant along the undulator in the definition of the dimensionless field strength $|a|$, and is not followed self-consistently. The optical field strength $|a|$ explains why stronger optical fields produce rapid electron evolution and, how more relativistic electrons, with a larger γ , require a stronger optical field E to accomplish the same bunching. When an electron loses energy, the value of $|a|$ increases so that the coupling between ζ and v increases. When more than 10% of the electron beam energy is converted to radiation, the FEL dynamics can be altered so that the more complete wave and pendulum equations may be used.

III. BEAM QUALITY AND GAIN EVOLUTION

A. THE FEL INTEGRAL EQUATION

To describe the FEL classically, the electron dynamics are governed by the optical wave (6) and electron pendulum (10) equations. In the case of weak fields, $|a| \ll \pi$, FEL dynamics can be expressed in the form of an integral equation by solving the electron pendulum and optical wave equations self-consistently [1, 5-7],

$$\dot{a}(\tau) = \frac{ij}{2} \int_0^\tau d\tau' \tau' F(\tau') e^{-i v_0 \tau'} a(\tau - \tau') \quad , \quad (11)$$

where $F(\tau') = \int dq f(q) e^{-iq\tau'}$ is the characteristic function of the distribution $f(q)$, $f(q)$ is the distribution of initial electron phase velocities $v_i = v_0 + q$ about v_0 , and $\int f(q) dq = 1$. Note that $F(\tau')$ and $f(q)$ only depend on the electron beam's initial conditions with subsequent dynamics described exactly. The FEL integral equation (11) is generally solved numerically, and has a distinct advantage over simulations which must follow many tens of thousands of sampled electrons.

When the current is low, $j \leq \pi$, the field $a(\tau - \tau')$ can be approximated by the initial field $a(0) = a_0$ in the integrand of (11). In the case of perfect beam quality, $f(q) = \delta(0)$ and $F(\tau') = 1$, the field at the end of the undulator $a(1)$ is easily evaluated to find the spectrum for low-gain,

$$G(v_0) = j [2 - 2\cos(v_0) - v_0\sin(v_0)] / v_0^3 \quad (12)$$

where gain is defined as $G = (a^2(1) - a_0^2) / a_0^2$. The antisymmetric shape of the low-gain spectrum has width $\Delta v_0 \approx 2\pi$ and a peak value $G \approx 0.13j$ at $v_0 \approx 2.6$. These features are among the first FEL characteristics found experimentally [1].

When the current is high, $j \gg \pi$, the optical field grows exponentially and at resonance, $v_0 = 0$, where the growth rate is maximum, the gain is $G(\tau) \approx \exp((j/2)^{1/3}\sqrt{3}\tau) / 9$. Near resonance, $v_0 \approx 0$, the final gain at $\tau = 1$ is

$$G(v_0) \approx \exp(\sqrt{3}(j/2)^{1/3}) (1 - v_0^2/3\sqrt{3}(j/2)^{1/3}) / 9 \quad (13)$$

The gain spectrum for high current is symmetric about resonance, and drops off at a characteristic value of the phase velocity $\Delta v_0 \approx 2(3\sqrt{3})^{1/2}(j/2)^{1/6} \approx 4.22j^{1/6}$. For large j , say $j \approx 30$, the peak gain, $G = \exp(\sqrt{3}(j/2)^{1/3})/9 \approx 8$ is much larger over a broader spectrum, $\Delta v_0 = 7.5$, than in the low-gain case.

B. ELECTRON DISTRIBUTION FUNCTIONS

Many experiments do not have the perfect beam quality used in the analytic results (12) and (13). Depending on specific experimental conditions, the actual shape of the electron beam distribution function may vary from one experiment to another. An initial electron phase velocity $v_i = L[(k + k_0)\beta_z(0) - k]$ depends on the initial electron z velocity $c\beta_z(0)$, and is therefore a function of both the energy spread and angular spread in the beam. Consider a relativistic electron beam with average energy γmc^2 ,

and spread described by width $\sigma_G = 4\pi N \Delta\gamma/\gamma$. The resulting distribution to be used in the integral equation (11) is the *Gaussian* distribution [5-7],

$$f(q) = \frac{e^{-q^2/2\sigma_G^2}}{\sqrt{2\pi}\sigma_G} \quad \text{for all } q. \quad (14)$$

Alternatively, an angular spread caused by emittance in the beam can result in the exponential distribution for $f(q)$. A relativistic electron entering the undulator with velocity $c\beta_0$ at a small angle θ has a reduced z velocity, $c\beta_z \approx c\beta_0 \cos\theta \approx c\beta_0(1-\theta^2/2)$, and the corresponding change in the phase velocity, $v(\theta) \approx v_0 - 2\pi N \gamma^2 \theta^2/(1+K^2)$. A Gaussian spread in angles θ of width $\Delta\theta$ results in the *exponential* distribution [5-7],

$$f(q) = \frac{e^{-q/\sigma_\theta}}{\sigma_\theta} \quad \text{for } q \leq 0 \quad \text{and} \quad f(q) = 0 \quad \text{for } q > 0, \quad (15)$$

where $\sigma_\theta = 4\pi N \gamma^2 \Delta\theta^2/(1+K^2)$. If a very broad angular distribution is cutoff by an emittance filter, the resulting phase velocity spread is a *triangular-shaped* distribution with positive slope [7],

$$f(q) = \frac{2}{\sigma_+^2}(\sigma_+ + q) \quad \text{for } -\sigma_+ \leq q \leq 0 \quad \text{and} \quad f(q) = 0 \quad \text{otherwise}, \quad (16)$$

where σ_+ is the width of the triangle.

In a realistic FEL, the correct shape of $f(q)$ is generally not known precisely, and is determined by several complicating factors involving the accelerator and electron beam transport properties. The $L = 5\text{m}$ Paladin experiments are taken to be described by the Gaussian distribution (14), whereas the $L = 15\text{m}$ Paladin experiments made use of an emittance filter

and transport system that resulted in a distribution more like (16) or possibly (15).

C. GAIN SPECTRUM BROADENING IN THE 5 m PALADIN

As the LLNL Paladin experiment developed, measurements were made with undulators of first 5 m and then later 15 m length [2-4]. In the 5 m experiment, the electron beam current was about 600 A at about $\gamma mc^2 = 41$ MeV energy and had a radius of $r_b \approx 5$ mm. The $L = N\lambda_0 = 5$ m undulator contained $N \approx 62$ periods of wavelength $\lambda_0 = 8$ cm, and undulator parameter $K = 0.9$. The radiation wavelength was $\lambda \approx 10.6$ μ m in a radiation mode with waist $w_0 \approx 4$ mm that was slightly smaller than the electron beam radius $r_b \approx 5$ mm at the beginning of the undulator so that it reduced the effective current density. Natural diffraction allows the optical mode to expand, and we determine the filling factor F in j by averaging along the undulator. As a result, we describe the 5m Paladin experiment by dimensionless current $j \approx 30$. The observed electron beam brightness establishes that the spread in initial phase velocities is about $\Delta v_0 \approx 12$, but the shape of the distribution is not known. We take the shape to be the Gaussian distribution as described in (14) with $\sigma_G = 12$.

In figure 1, the weak-field gain spectrum (shown as dots) was measured by varying the undulator field strength B over a small range to change the resonance condition v_0 [5-7]. The observed gain spectrum width is $\Delta v_0 \approx 40$, with peak gain of $G \approx 12\%$. The solid curve uses the integral equation to evaluate gain with $j = 30$ and $\sigma_G = 12$. The theoretical gain spectrum was

observed to be antisymmetric in shape with a peak gain of $G \approx 0.15$. The observed and theoretical gain spectra are dramatically distorted by the effects of poor beam quality. Figure 2 shows, for comparison, the gain spectrum determined by the integral equation with $j = 30$ and $\sigma_G = 0$ describing perfect beam quality. Poor beam quality is responsible for decreasing the FEL peak gain from $G \approx 9$ in figure 2 to $G \approx 15\%$ in figure 1, and distorting the gain spectrum from an approximately symmetric shape of width $\Delta v_0 \approx 6$ to an antisymmetric shape of width $\Delta v_0 \approx 70$. Note that the observed and theoretical antisymmetric spectra in figure 1 are both much broader than the antisymmetric low-gain spectral shape in (12) with width $\Delta v_0 \approx 2\pi$.

The shape, overall width, and peak value of the 5m Paladin gain spectrum is dramatically altered from the idealized gain spectrum (either (12) or in figure 2), and in this case, is determined by the initial distribution of electron velocities (14).

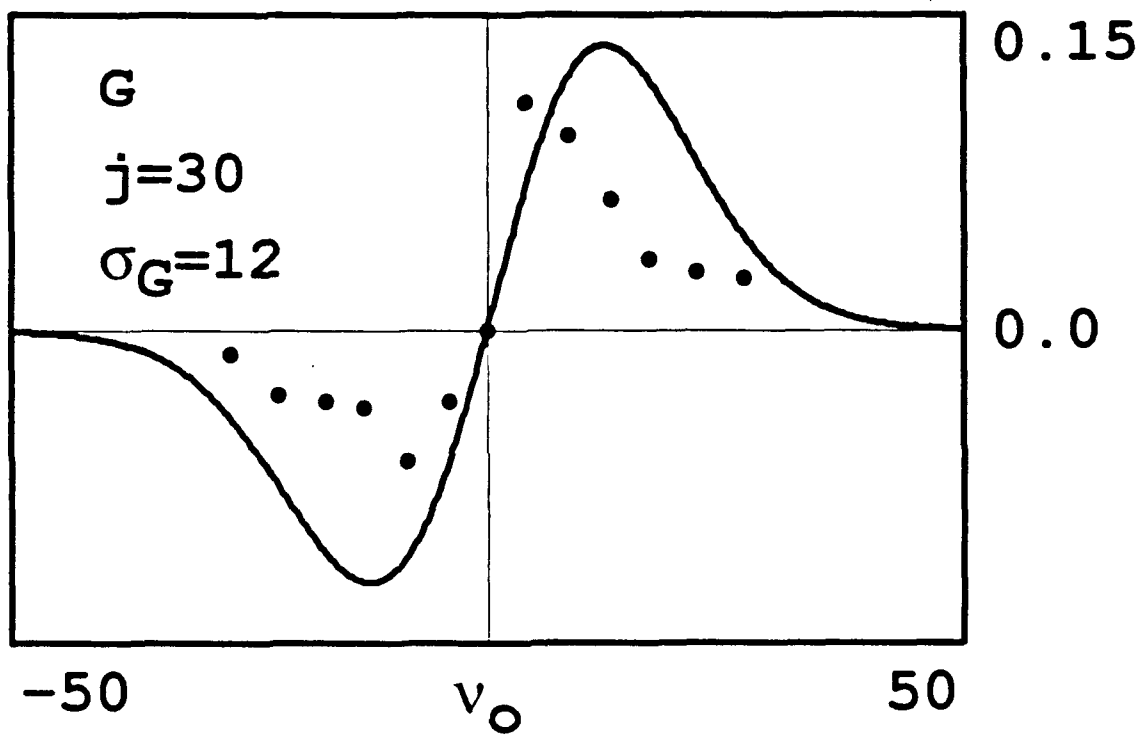


Figure 1. Gain evolution of the 5 m Paladin with poor beam quality

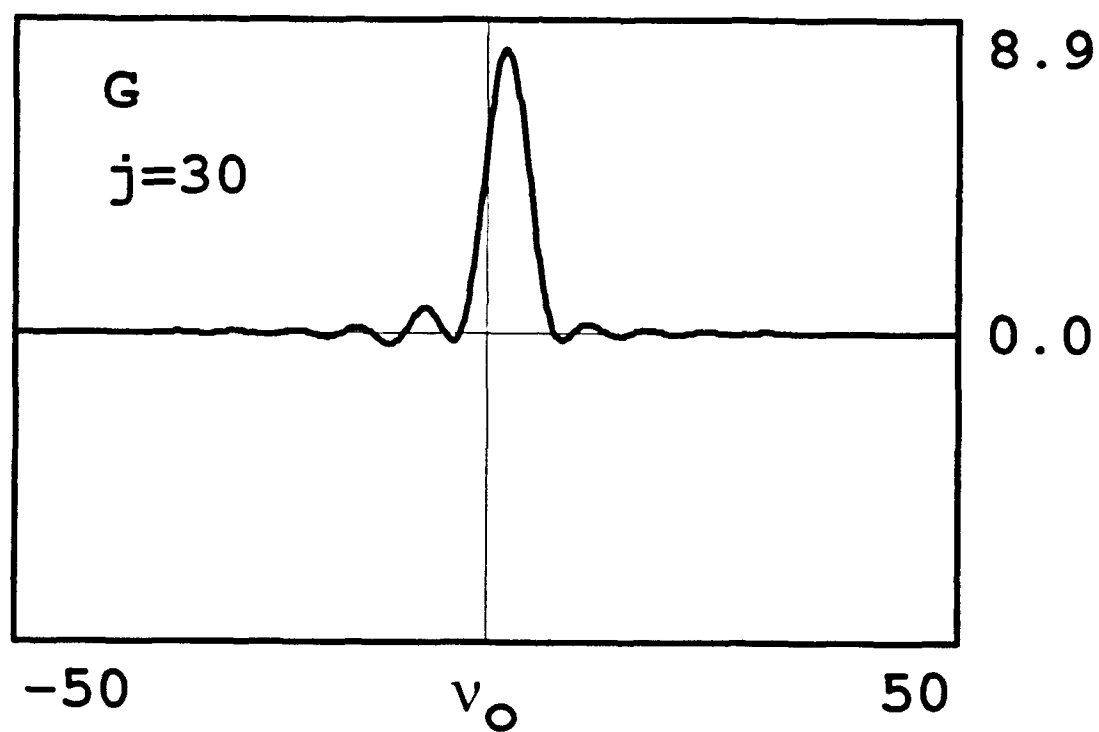


Figure 2. Gain evolution of the 5 m Paladin with ideal beam quality

D. A PLATEAU IN THE GAIN EVOLUTION OF THE 15 m PALADIN

We also identify characteristics of the Paladin 15m experiments that are unique to the initial electron distribution function shape. An emittance filter was used to improve the beam quality entering the undulator, and a detailed study of the filter and transport system concluded [13] that the distribution function shape should look something like the exponential or triangular distributions, (15) or (16).

In the 15 m experiment, the electron beam current was about 500 A at $\gamma mc^2 \approx 45$ MeV energy. The longer undulator was $L = 15$ m long, containing $N \approx 187$ periods with $K = 1.0$. The high gain observed in the 15 m experiment causes the optical mode and electron beam to be well matched over the whole undulator length, so that we take $F \approx 1$. Other parameters are the same as in the 5 m experiment. Because of the longer undulator length, the 15 m experiment is described by large $j \approx 1400$, and the triangular distribution (16) with $\sigma_+ \approx 13$. For such a large current, the ideal gain, with perfect beam quality, $\sigma_+ = 0$, would be $G \approx 5 \times 10^5$ peaked at $\nu_0 = 0$ and would evolve exponentially in τ . Figure 3 shows the theoretical gain evolution, $G(\tau)$, found by solving the integral equation with the triangular-shaped distribution (16) of width $\sigma_+ = 13$, $j = 1400$, and $\nu_0 = 0$. The gain evolution, $G(\tau)$, represents the optical power growth along the undulator length as τ goes from 0 to 1, and it shows a dramatic plateau about half way along the undulator from $\tau \approx 0.5$ to 0.7. The choice of an exponential distribution (15) shows significantly smaller gain than the triangular-shaped distribution and with a more subtle plateau.

Figure 4 shows the optical power, P , measured along the 15 m undulator length [2], corresponding to $\tau = 0 \rightarrow 1$. The changes in power indicate the gain evolution, and the figure shows a the prominent plateau in the middle of interaction length. It appears that the shape of the distribution function in the Paladin 15 m experiment has resulted in a plateau in the FEL interaction half way through the undulator, and the experimental plateau in the gain evolution is verified by the integral equation with the positive sloped triangular-shaped distribution.

In conclusion, the results of the Paladin 5 m and 15 m experiments, have provided a unique opportunity to observe how the FEL gain spectrum and gain evolution can be determined by the electron beam velocity distribution instead of the natural high-gain mechanism. The measurements provide the first comparison between theory and experiment in a short-wavelength device where the electron beam distribution plays a dominant role in the FEL mechanism. The gain spectrum shape, width, and evolution can be used to determine unique information about beam quality.

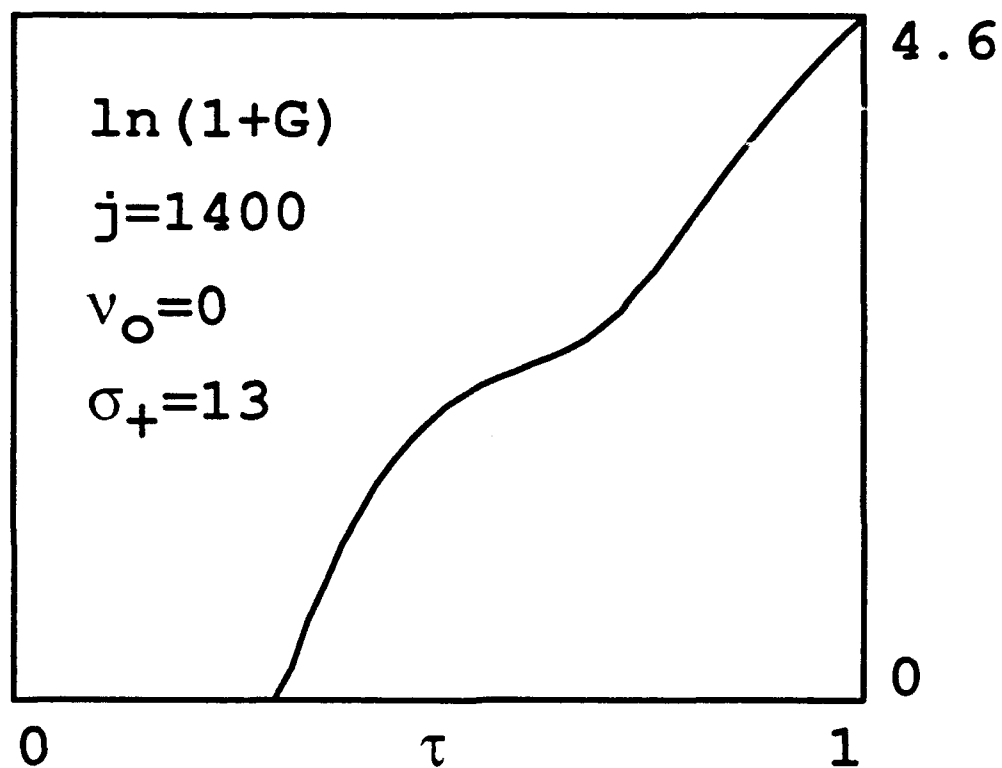


Figure 3. Theoretical gain along the 15 m Paladin undulator

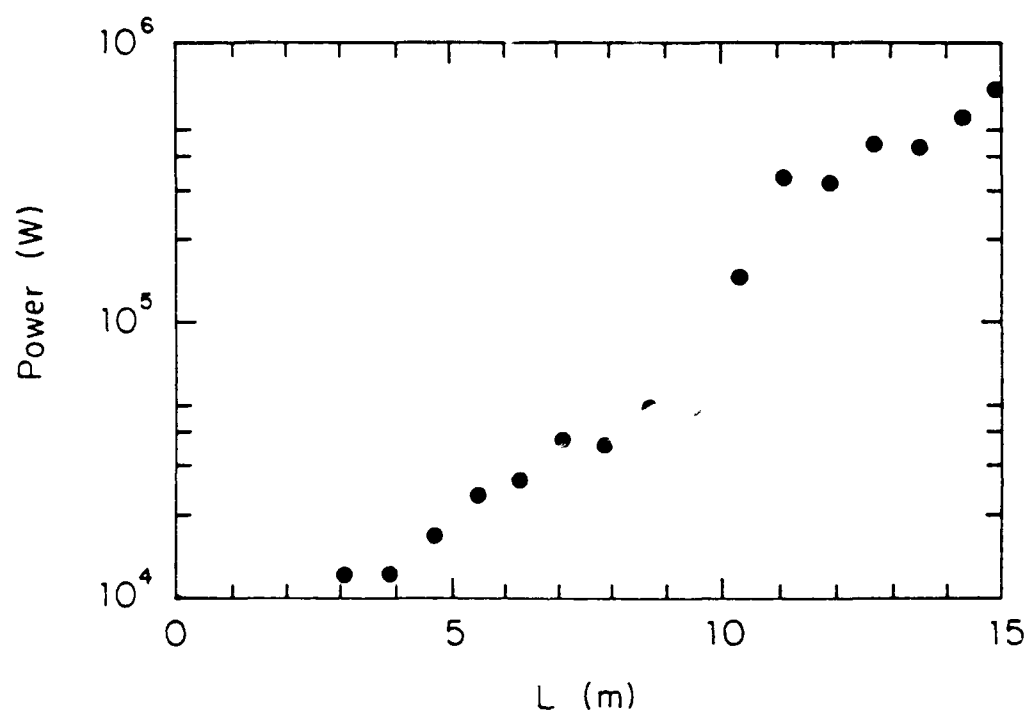


Figure 4. Experimental gain along the 15 m Paladin undulator

IV. A SIMPLE MODEL OF THE ELF FEL

A. DESCRIPTION OF ELF EXPERIMENT

The LLNL Electron Laser Facility (ELF) FEL is an amplifier with very high gain operating in the microwave regime using the Experimental Test Accelerator (ETA). The experiment examined high-power saturation, and the effect of tapering the undulator field. ETA uses a 6 kA electron beam with a normalized emittance of 1.5π cm-rad [8]. An emittance filter reduces the beam current to approximately 450 A over a pulse length of 15 ns with normalized edge emittance of 0.47π cm-rad. The beam energy is 3.3 MeV with $\gamma = 7.5$. The electron beam particle density is $\rho \approx 2 \times 10^{11}$ cm⁻³, and the beam radius is $r_b = 4$ mm.

The $L = 3$ m long ELF undulator is linearly polarized, with wavelength $\lambda_0 = 9.8$ cm and undulator constant $K \approx 2.8$. The peak field strength is $B \approx 4300$ G over $N = 30$ undulator periods. The Rayleigh length is less than 1% of the undulator length so that ELF must use a $3 \text{ cm} \times 10 \text{ cm}$ rectangular waveguide to confine the radiation wavefront around the electron beam for continued amplification. Without a waveguide, natural diffraction would spread the optical wave cross-section away from the amplifying electron beam and reduce coupling. The waveguide cutoff frequency is 5 GHz in the TE_{01} mode, so that the FEL at 35 GHz operates

far above cutoff.

B. SIMPLE FEL EQUATIONS FOR ELF EXPERIMENT

The FEL equations described in previous chapters are the self-consistent pendulum and wave equations. They provide a simple model of the FEL that is valid in strong and weak optical fields for high and low beam current. The assumptions required to derive the simple form of the equations are $\gamma \gg 1$ and $N \gg 1$. Since the most important aspects of the interaction take place near resonance, the changes in the electron energy, $\Delta\gamma/\gamma$, are small when $N \gg 1$, and the FEL efficiency is low. For high efficiency, in the tapered undulator or in a short undulator with few periods, the changes in the electron energy are expected to be large. High efficiency FELs the undulator can be tapered to maintain resonance with the trapped electrons that lose energy to the optical wave. The untrapped electrons will drift far off-resonance. Tapering and high-efficiency can be added to the basic FEL electron equation of motion (10), and it becomes [14, 15]

$$\ddot{\zeta} = \dot{v} = \theta(|a| - a_s)\delta + (1 - (3v / 4\pi N))|a| \cos(\zeta + \phi) \quad , \quad (17)$$

where $\theta(x)$ is the step function, $\theta(x) = 0$ for $x < 0$ and $\theta(x) = 1$ for $x > 0$, so that the tapering starts at the onset of saturation, $a_s \approx 2(j / 2)^{2/3}$ is the saturation field, $\delta \approx 4\pi N \Delta\gamma_r / \gamma_r$ is the taper rate ($\delta = 0$ for the untapered undulator), and γ_r is the resonant Lorentz factor. The modified pendulum equation (17) relaxes the assumption of $N \gg 1$, but still assumes $\gamma \gg 1$ and allow tapering of the undulator.

In order to have a self-consistent theory, the dimensionless single-mode wave equation is also altered to account for high efficiency in terms of the electron phase and phase velocity [14, 15],

$$\dot{a} = -j < (1 - (v / 4\pi N)) e^{-i\zeta} > . \quad (18)$$

In these formulations, electrons near resonance, $v \approx 0$, are described accurately, while untrapped electrons far from resonance, $v \rightarrow 4\pi N$, are handled less accurately. However, the untrapped electrons are expendable since they become randomly spread in phase as well as uncoupled from the bunching interaction. For electrons near resonance, the bunching rate is determined by the field strength $|a|$. When $|a| \ll \pi$, the optical field is considered weak, and bunching is small. When $|a| \gg \pi$, i.e., the optical field is strong, the electrons bunch rapidly, and become trapped in closed phase-space orbits. The current j determines the coupling between the electron beam and the optical wave. Without current, $j = 0$, or no bunching $\langle \dots \rangle = 0$, there is no change in the initial optical field, $a(0) = a_0$. The modified pendulum equation (17) and wave equation (18) are valid for weak fields, strong fields, low gain, high gain, tapered, untapered, low efficiency, and high efficiency, but assume $\gamma \gg 1$.

In a linearly-polarized undulator, each electron experiences fast, periodic oscillations that are comparable to the radiation wavelength and modify the interaction strength. For this coupling [1], the dimensionless current density j should include the factor $(J_0(\xi) - J_1(\xi))^2 = 0.54$ where $\xi = K^2 / 2(1 + K^2) = 0.44$ for ELF. For early ELF experiments with 450 A

beam current [9], the filling factor is $F = 0.026$, and the corrected current is $j = 3015$.

A relativistic electron in a rectangular waveguide far above cutoff has its phase velocity shifted by [1]

$$\Delta v_{pq} \approx - \frac{\pi N \lambda_0^2 (1 + K^2)}{8 \gamma^2} \left[\frac{p^2}{X^2} + \frac{q^2}{Y^2} \right] , \quad (19)$$

where X is the long waveguide dimension, Y is the short waveguide dimension, and p and q are integers. For ELF in the TE_{01} mode, the resonant phase velocity is shifted by $\Delta v_{01} \approx -6\pi$. A change in the undulator field, δB , about the resonant field strength B_0 also causes a change in phase velocity by

$$\Delta v_B \approx - \frac{4\pi N K^2}{(1 + K^2)} \frac{\delta B}{B_0} . \quad (20)$$

Resonance in the ELF FEL is tuned using changes in the magnetic field $\delta B / B_0$ [8]. Combining (19) and (20) shows that the waveguide increases the resonant undulator field strength by $\Delta B_{01} \approx 240$ G.

The distribution of initial phase velocities, $f(v)$, is important to the FEL growth rate and in ELF is determined by the electron beam emittance filter. The emittance filter results in a triangular-shaped distribution function with a positive slope given by

$$f_+(v) = (v - v_0 + 2\sigma_+) / 2\sigma_+^2 , \quad \text{for } v_0 - 2\sigma_+ \leq v \leq v_0 ,$$

where v_0 is the peak of the beam distribution. The full-width at the base of the triangle is equivalent to a 6.4% energy spread so that $2\sigma_+ =$

$4\pi N \times 0.064$, and $\sigma_+ \approx 12$ [10]. The initial input power in ELF is 30 kW in the TE_{01} waveguide mode, and corresponds to a dimensionless microwave field magnitude of $\alpha_0 = 12$.

C. RESULTS

Figure 5 shows the simulated gain spectrum, $G(v_0)$, and figure 6 shows the experimental result, $G(\Delta v_B)$, at the end of the undulator. Recall that the equation (20) shows the relationship between the change in v_0 used in the simulation and the change in the magnetic field used in the experiment. The data is taken with $I = 450$ A beam current so that $j = 3015$, and $\sigma_+ = 12$ [9]. The simulation gives peak gain $G_{\max} \approx 2833$ at $\Delta v_0 \approx 28$ away from resonance with a gain bandwidth of $\delta v_0 \approx 30$. The observed peak gain is four times higher than the calculated result, and is shifted from resonance more than in the simulation. However, the important qualitative features of the experiment are shown by the simple single-mode theory. The asymmetrical gain spectrum shape is in good agreement. Mode distortion by excitation of higher-order waveguide modes probably accounts for the some of higher measured gain, and the larger shift away from resonance in the experiment. Some of the disagreement may also be due to experimental error, since the powerful microwave pulse must be attenuated by many orders of magnitude before a measurement can be made.

The extraction of higher-order modes has the effect of confining the microwave power around the electron beam, increasing the effective filling factor, and increasing coupling in the later parts of the undulator. In order to account for mode distortion, we increase the filling factor from 0.026 to 0.032. Figure 7 shows the simple simulation results for power evolution, $P(\tau)$, and figure 8 shows the experiment results for power evolution, $P(z)$. The later ELF experiments increase the current to 850 A [10, 11] so that the dimensionless current density with the new filling factor is now $j = 7000$. The dimensionless microwave field is $a_0 = 15$, and $\sigma_+ = 12$. The onset of saturation occurs at $\tau \approx 0.5$, or about 1.5 m along the undulator, and the efficiency is $\eta \approx 5\%$ in the untapered case. The shape of $P(\tau)$ in the untapered case in figure 7 and figure 8 shows excellent agreement between the simple theory and experiment.

In order to extend the natural saturation limit, the undulator properties can be altered along z to maintain resonance and interaction strength. The phase acceleration, δ , is given by $\delta \approx -4\pi NK^2 \Delta B / B_0(1 + K^2)$ when the undulator field strength is decreased by ΔB [16]. Figure 7 shows the result of tapering with $\delta = 90\pi$ giving an efficiency of $\eta \approx 31\%$. The experimental results in figure 8 shows that the efficiency is increased from 6% to 35%, because of tapering [11]. The efficiency is increased by about a factor of six in both simulation and the experiment. In both cases, tapered and untapered, we see excellent agreement between the experiment and the

simplified simulation .

In each comparison above, the excitation of higher-order waveguide modes confines the microwave field tightly around the electron so that the filling factor F and the coupling are effectively increased. The ELF experiments determined that about 30% of the microwave power is in higher-order modes [10], consistent with this model.

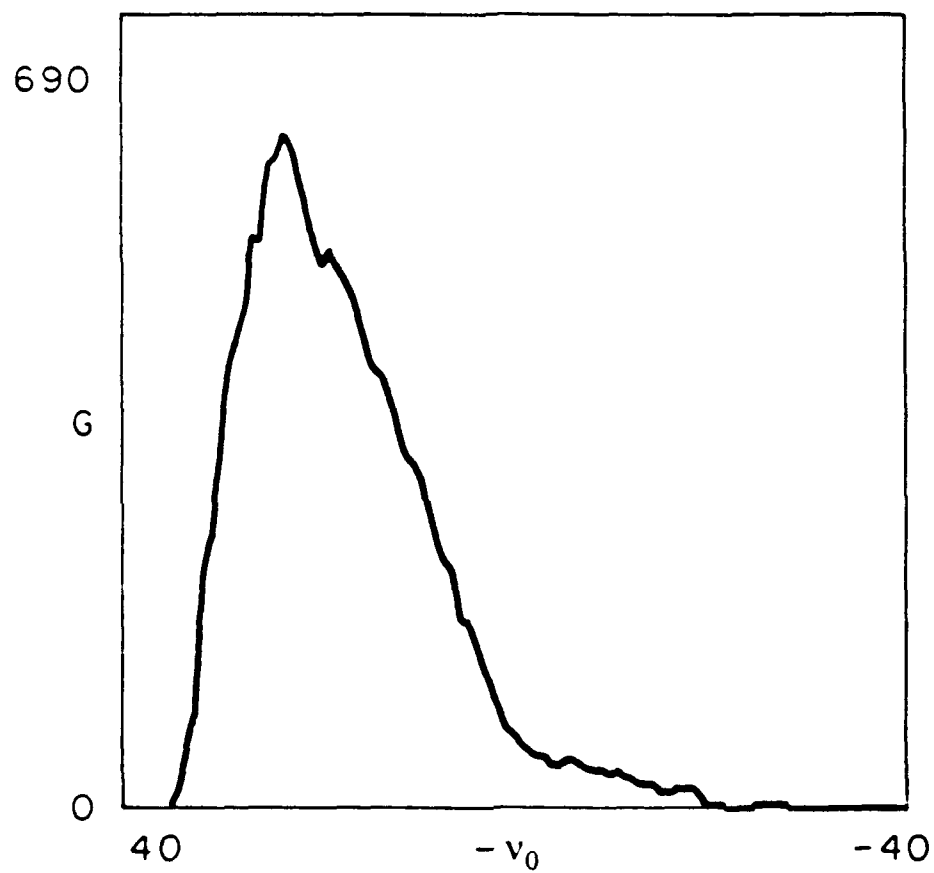


Figure 5. Simulated gain spectrum

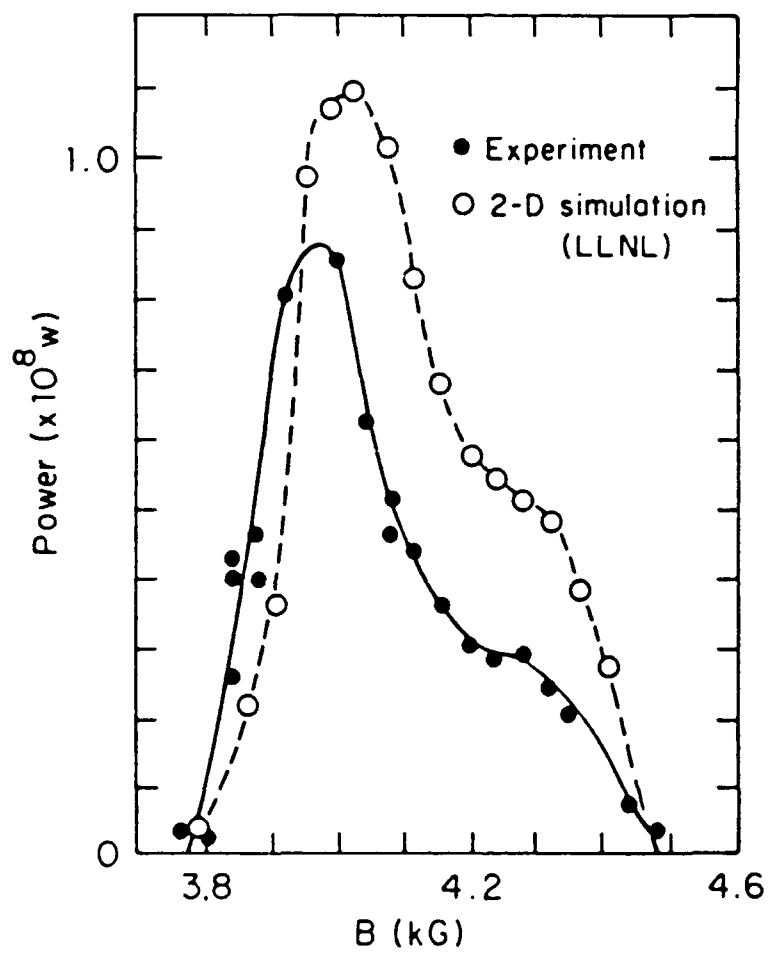


Figure 6. Gain spectrum of the ELF experiment

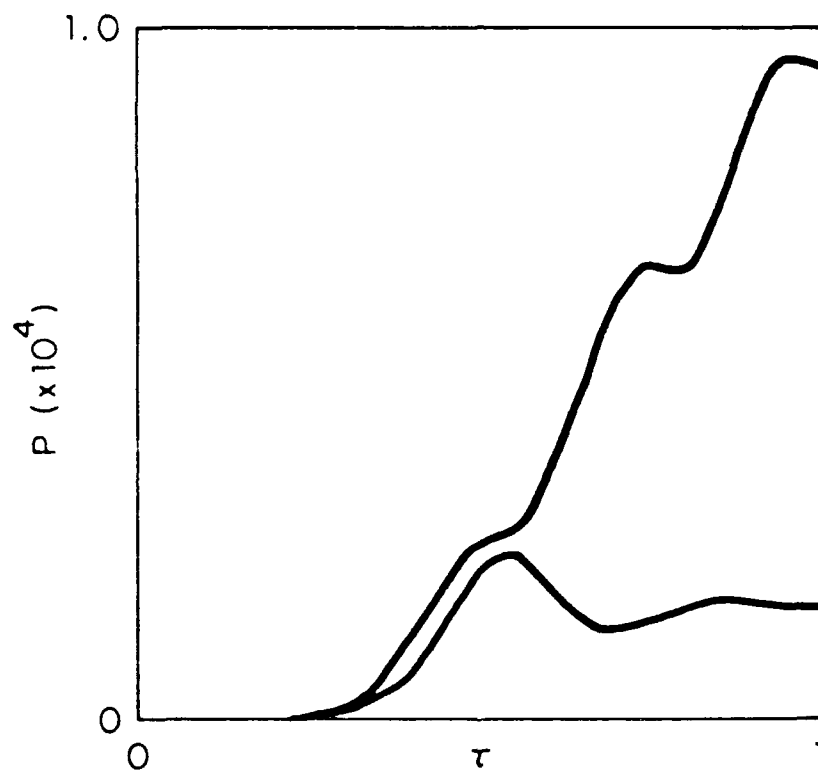


Figure 7. Simulated gain evolution along the undulator

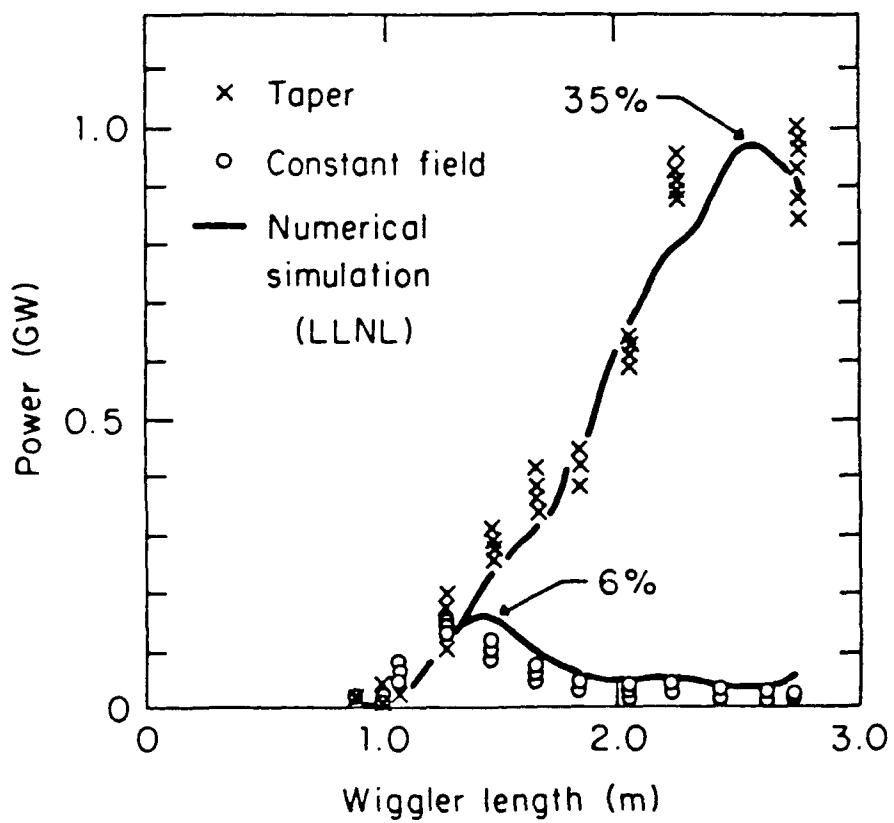


Figure 8. Gain evolution of ELF experiment

LIST OF REFERENCES

- [1] W. B. Colson, "Classical Free Electron Laser Theory", Chapter 5 in *Free Electron Laser Handbook*, W. B. Colson, C. Pellegrini and A. Renieri (editors), North-Holland Physics, Elsevier Science Publishing Co. Inc., The Netherlands (1990).
- [2] T. J. Orzechowski, "Paladin - A 10.6- μ m Free Electron Laser Amplifier", Beijing Inst. of Mod. Phys. Vol 2, World Scientific, 207 (1989).
- [3] T. J. Orzechowski, and others, "Free-Electron Laser Results from the Advanced Test Accelerator", 1988 LINAC Conference Proceedings, CEBAF-Report-89-001, CEBAF Newport News, 281 (1989).
- [4] T. J. Orzechowski, "Free-Electron Lasers Driven by Linear Induction Accelerators", UCRL-JC-105563, LLNL, (1990).
- [5] W. B. Colson, J. C. Gallardo, and P. M. Bosco, "Free-Electron Laser Gain Degradation and Electron Beam Quality", Physical Review **A34**, 4875 (1986).
- [6] W. B. Colson and J. Blau, "Free Electron Laser Theory in Weak Optical Fields", Nuclear Instruments and Methods in Physics Research **A259**, 198-202 (1987).
- [7] J. Blau and W. B. Colson, "The Effects of Electron Beam Quality on the Free Electron Laser Mechanism", accepted by Nuclear Instruments and Methods in Physics Research (1991).
- [8] T. J. Orzechowski, and others, "Microwave Radiation from a High-Gain Free-Electron Laser Amplifier", Physical Review Letters **54**, 889 (1985).

- [9] T. J. Orzechowski, and others, "High-Gain Free Electron Laser Using Induction Linear Accelerators", IEEE Journal of Quantum Electronics **QE-21**, 831 (1985).
- [10] E. T. Scharlemann, and others, "Comparison of the Livermore Microwave FEL Results at ELF with 2D Numerical Simulation", Nuclear Instruments and Methods in Physics Research **A250**, 150 (1986).
- [11] T. J. Orzechowski, and others, "High-Efficiency Extraction of Microwave Radiation from a Tapered-Wiggler Free-Electron Laser", Physical Review Letters **57**, 2172 (1986).
- [12] J. D. Jackson, *Classical Electrodynamics*, Wiley, New York, (1975).
- [13] E. T. Scharlemann, Private Communication
- [14] W. B. Colson, "The Trapped-Particle Instability in Free Electron Laser Oscillators and Amplifiers", Nuclear Instruments and Methods in Physics Research **A250**, 168 (1986).
- [15] J. -H. Park and W. B. Colson, "A Simple Model of the LLNL ELF FEL Amplifier", accepted by Nuclear Instruments and Methods in Physics Research (1991).
- [16] W. B. Colson, "Fundamental free electron laser theory and new principles for advanced devices", SPIE **78**, 2 (1987).